Insulin regulates carboxypeptidase E by modulating translation initiation scaffolding protein eIF4G1 in pancreatic β cells

Chong Wee Liew[a,b,1,2], Anke Assmann[a,1], Andrew T. Templin[c], Jeffrey C. Raum[d], Kathryn L. Lipson[e,3], Sindhu Rajan[f], Guifen Qiang[b], Jiang Hu[a], Dan Kawamori[a], Iris Lindberg[g], Louis H. Philipson[f], Nahum Sonenberg[h], Allison B. Goldfine[a], Doris A. Stoffers[d], Raghavendra G. Mirmira[c], Fumihiko Urano[i], and Rohit N. Kulkarni[a,2]

[a]Joslin Diabetes Center and Department of Medicine, Brigham and Women's Hospital, Harvard Medical School, Boston, MA 02215; [b]Department of Physiology and Biophysics, University of Illinois at Chicago, Chicago, IL 60612; [c]Department of Cellular and Integrative Physiology, Indiana University School of Medicine, Indianapolis, IN 46202; [d]Department of Medicine/Endocrinology, Diabetes, and Metabolism and the Institute for Diabetes, Obesity, and Metabolism, Perelman School of Medicine at the University of Pennsylvania, Philadelphia, PA 19104; [e]Program in Gene Function and Expression, University of Massachusetts Medical School, Worcester, MA 01605; [f]Department of Medicine, The University of Chicago, Chicago, IL 60637; [g]Department of Anatomy and Neurobiology, University of Maryland, Baltimore, MD 21201; [h]Department of Biochemistry, McGill University, Montreal, QC, Canada H3A 1A3; and [i]Division of Endocrinology, Metabolism, and Lipid Research, Department of Medicine, Washington University School of Medicine, St. Louis, MO 63110

Insulin resistance, hyperinsulinemia, and hyperproinsulinemia occur early in the pathogenesis of type 2 diabetes (T2D). Elevated levels of proinsulin and proinsulin intermediates are markers of β-cell dysfunction and are strongly associated with development of T2D in humans. However, the mechanism(s) underlying β-cell dysfunction leading to hyperproinsulinemia is poorly understood. Here, we show that disruption of insulin receptor (IR) expression in β cells has a direct impact on the expression of the convertase enzyme carboxypeptidase E (CPE) by inhibition of the eukaryotic translation initiation factor 4 gamma 1 translation initiation complex scaffolding protein that is mediated by the key transcription factors pancreatic and duodenal homeobox 1 and sterol regulatory element-binding protein 1, together leading to poor proinsulin processing. Reexpression of IR or restoring CPE expression each independently reverses the phenotype. Our results reveal the identity of key players that establish a previously unknown link between insulin signaling, translation initiation, and proinsulin processing, and provide previously unidentified mechanistic insight into the development of hyperproinsulinemia in insulin-resistant states.

ER stress | prohormone | bIRKO | GWAS

Elevated proinsulin and processing intermediates in the circulation of patients with type 2 diabetes (T2D) suggest a defect in hormone processing in β-cell secretory granules (1–3). Genome-wide association studies have recently identified several SNPs in or near the *TCF7L2*, *SLC30A8*, *SGSM2*, *VPS13C*, MAPK-activating death domain (*MADD*), and *ADCY5* genes that are associated with either altered proinsulin levels or proinsulin-to-insulin conversion (4–6). These findings gain significance because an increase in the proinsulin-to-insulin ratio predicts future development of T2D in apparently healthy individuals (7, 8). Given that proinsulin has only ~5% of the biological activity of mature insulin, an increase in circulating proinsulin is predicted to limit the actions of mature insulin and, consequently, to contribute to worsening glucose tolerance in humans (9). Other studies have reported increased circulating proinsulin in insulin-resistant obese subjects with normal glucose tolerance compared with nonobese individuals (10, 11), suggesting a potential role for insulin resistance in proinsulin processing. However, the precise molecular mechanisms underlying β-cell dysfunction that promote hyperproinsulinemia remain poorly understood.

The biosynthesis of insulin is regulated at multiple levels, including transcription as well as posttranslational protein folding at the endoplasmic reticulum (ER) and proteolytic cleavage and modification of the properly folded proinsulin in the secretory granules by prohormone convertase (PC) 1/3, PC2, and carboxypeptidase E (CPE) (12–16). However, the effects of insulin signaling on posttranslational processing of insulin are not fully explored.

In addition to insulin's actions in classical insulin-responsive tissues (muscle, liver, and fat), insulin signaling regulates β-cell mass and function (17–22), as well as transcription of the insulin gene itself (23). We hypothesized that disruption of normal growth factor (insulin) signaling in the β cell has an impact on proinsulin processing and/or adversely affects the function of the ER and, ultimately, the β cell. In this study, to examine whether disruption of the insulin-signaling pathway has a direct impact on proinsulin content, we examined the pancreas and islets from

Significance

Elevated circulating proinsulin and a poor biological response to insulin are observed early in individuals with type 2 diabetes. Genome-wide association studies have recently identified genes associated with proinsulin processing, and clinical observations suggest that elevated proinsulin and its intermediates are markers of dysfunctional insulin-secreting β cells. Here, we propose a previously unidentified mechanism in the regulation of an enzyme that is involved in proinsulin processing called carboxypeptidase E (CPE). Disruption of insulin signaling in β cells reduces expression of a scaffolding protein, eukaryotic translation initiation factor 4 gamma 1, that is required for the initiation of translation and occurs via regulation of two transcription factors, namely, pancreatic and duodenal homeobox 1 and sterol regulatory element-binding protein 1. Together, these effects lead to reduced levels of CPE protein and poor proinsulin processing in β cells.

mice with insulin receptor knockout in the β cells (βIRKO), a mouse model manifesting a phenotype that resembles human T2D (19), and we also investigated β-cell lines lacking the insulin receptor (IR) (20). We have previously reported that βIRKO mice developed age-dependent, late-onset T2D (19) with an increase in the ratio of circulating total insulin to C-peptide suggesting elevated proinsulin secretion by βIRKO cells. However, the potential contribution of proinsulin in the development of T2D remains unknown.

We demonstrate an increased accumulation of proinsulin in the βIRKO cells due to altered expression of PC enzymes, especially CPE. These changes are mediated by duodenal homeobox protein (Pdx1) and sterol regulatory element-binding protein 1 (SREBP1) transcriptional regulation of the translation initiation complex scaffolding protein, eukaryotic translation initiation factor 4 gamma (eIF4G) 1, and indicate a previously unidentified role for these transcription factors in the regulation of translational initiation. Reexpression of the IR in the βIRKO cells, knocking down proinsulin, or maintaining normal expression of CPE each independently restores the normal phenotype in mutant β cells. Together, these data point to previously unidentified links between insulin signaling, translational initiation, and proinsulin processing.

Results

Lack of IRs in β Cells Promotes Proinsulin Accumulation. To investigate the role of proinsulin in the development of diabetes in βIRKO mice, we performed longitudinal studies in control and βIRKO male mice fed a chow diet from the age of 2–7 mo. We observed that both control and βIRKO mice at the age of 4 mo exhibited an increase in the proinsulin/insulin ratio compared with their respective levels at 2 mo, despite unaltered fed blood glucose levels (Fig. 1A), and argue against the primary role of glucose in the modulation of proinsulin levels. Interestingly, we also observed that βIRKO mice manifested a much greater elevation in the proinsulin/insulin ratio beginning at the age of 4 mo until the end of the study, which was accompanied by elevated blood glucose when the mice were 5 mo old (Fig. 1A). Our data indicate that impaired insulin signaling in β cells increases circulating proinsulin and, notably, occurs before the onset of hyperglycemia. These data provide an association between hyperproinsulinemia and the development of T2D in the β-cell insulin signaling-deficient βIRKO model and prompted us to examine the direct role of insulin signaling in proinsulin processing in the β cells. Considering that the IR substrate-2 knockout (IRS2KO) mouse (24) phenocopies the βIRKO mouse, it is worth exploring whether the higher circulating insulin immunoreactivity in the former is also due, in part, to higher proinsulin levels.

To confirm that the elevated proinsulin is indeed derived from β cells, we examined the pancreas from control and βIRKO mice. Immunohistochemical analyses revealed high levels of proinsulin in a significantly greater number of β cells from the βIRKO mice compared with controls (Fig. 1B). Consistent with these data, cellular content of proinsulin and the proinsulin/insulin ratio were also significantly higher in the βIRKO islets, as determined by ELISA and HPLC (Fig. 1C and Fig. S1A). Furthermore, consistent with the observations in primary islets isolated from the βIRKO mice, β-cell lines lacking the IR (βIRKO) (20) also exhibited a significantly higher proinsulin/insulin ratio and proinsulin content (Fig. 1D and Fig. S1B). Based on these data, and given the limitations of using primary islets for mechanistic experiments, we focused on studying βIRKO cell lines.

To evaluate dynamic alterations in processing, we transfected control or βIRKO cell lines with an insulin–C-peptide–GFP construct. Western blotting of lysates from control cells, obtained 48 h after transfection, revealed the presence of proinsulin-GFP (Fig. 1E; 40 kDa), a fully cleaved C-peptide–GFP band (Fig. 1E; 30 kDa), and intermediate bands likely to be partially processed A or B chains
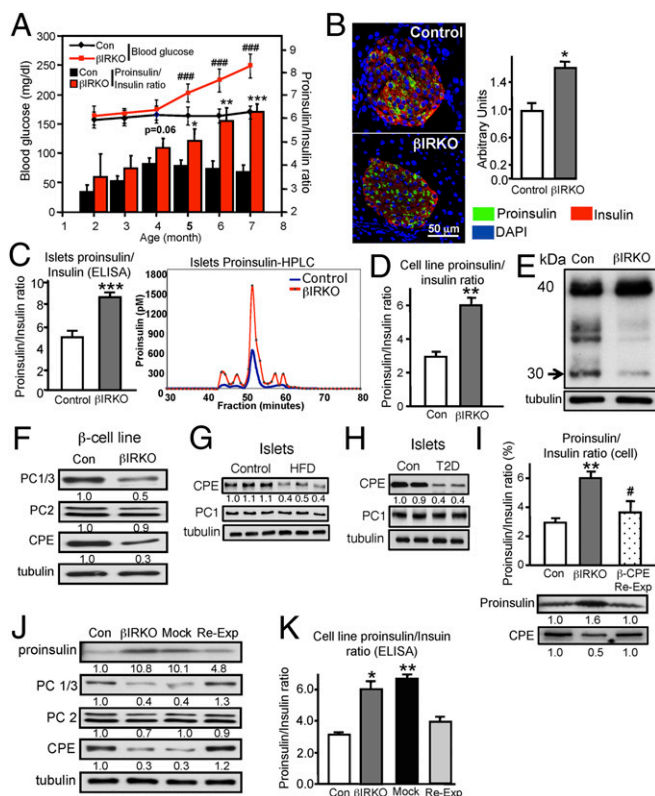

Fig. 1. Increase in proinsulin due to down-regulation of CPE in β cells lacking IRs. (A) Blood glucose and circulating proinsulin-to-insulin ratio in control (Con) or βIRKO mice aged 2–7 mo (n = 5–9). (B) Immunostaining and quantification for proinsulin (green), insulin (red), and DAPI (blue) in pancreas sections from control or βIRKO mice (n = 4–5). (Scale bar, 50 μm.) (C) Proinsulin-to-insulin ratio measured with ELISA and proinsulin content measured by HPLC in islets isolated from control or βIRKO mice using ELISA (n = 5–6). (D) Proinsulin-to-insulin ratio measured with ELISA in control or βIRKO cell lines (n = 4). (E) Western blotting for C-peptide–GFP in a control or βIRKO cell line expressing a preproinsulin-GFP expression construct (arrow points to C-peptide–GFP; n = 3 per group). (F) Western blotting for PC1/3, PC2, CPE, or tubulin (loading control) in a control or βIRKO cell line (n = 4). (G) Representative Western blotting for CPE, PC1/3, or tubulin (loading control) in islets (pooled) isolated from control or HFD-fed C57BL/6J mice (n = 6). (H) Representative Western blotting for CPE, PC1/3, or tubulin (loading control) in islets isolated from controls or patients with T2D (n = 5). (I) Proinsulin-to-insulin ratio measured with ELISA and Western blotting for CPE or proinsulin in control, βIRKO, or β-CPE–reexpressing (Re-Exp) cell lines (n = 4). **P < 0.01 (vs. control); #P < 0.05 (vs. βIRKO). (J) Western blotting for proinsulin, PC1/3, PC2, CPE, or tubulin (loading control) in control, βIRKO, mock, or Re-Exp β-cell lines (n = 3). (K) Proinsulin-to-insulin ratio measured with ELISA in control, βIRKO, mock, or Re-Exp β-cell lines (n = 4 per group). *P < 0.05; **P < 0.01; ***P < 0.001. Data are mean ± SEM.

attached to C-peptide GFP. In the βIRKO cells, we also observed the proinsulin-GFP precursor; however, in marked contrast to the controls, we detected significantly reduced fully cleaved C-peptide–GFP and also partially processed proinsulin-GFP intermediates, confirming poor processing of proinsulin. To investigate the underlying cause of poor proinsulin processing in βIRKO cells, we evaluated the expression pattern of the proinsulin processing enzymes PC1/3, PC2, and CPE. In both the cell line (Fig. 1F) and islets (Fig. S1C), we observed a significant decrease in the expression of processing enzymes, with the most striking reduction evident in the expression of CPE. Interestingly, we also observed a similar down-regulation of CPE protein in islets isolated from C57BL/6J mice fed a high-fat diet (HFD) (Fig. 1G), which is a commonly used T2D mouse model, as well as in primary human islets isolated from patients with T2D

(Fig. 1*H*). Thus, the processing defect in the mutant β cells is associated with reduced expression of proinsulin-processing enzymes and is consistently observed in both primary T2D human and mouse islets.

Next, to explore the effects of restoring CPE levels, we transiently reexpressed CPE in the βIRKO cells and observed that the proinsulin/insulin ratio and proinsulin content were restored to control levels, as shown by both ELISA and Western blotting analyses (Fig. 1*I* and Fig. S1*D*). Thus, our results demonstrated that the proinsulin-processing defect is largely due to the downregulation of CPE in the βIRKO cells. We subsequently examined the role of insulin signaling in the regulation of proinsulin-processing enzymes and proinsulin levels in βIRKO cells, by stably reexpressing the human IR B isoform (exon 11+) in the mutant β cells (23) (Fig. S1*E*), and observed that the expression of PC1/3 and CPE, as well as proinsulin levels, reverted to control levels (Fig. 1*J*). Consistently, the proinsulin/insulin ratio was also restored (Fig. 1*K*).

Altered Expression of Proinsulin-Processing Enzymes in β Cells from βIRKO Mice. To examine if insulin signaling directly modulates the expression of the processing enzymes, we stimulated control or βIRKO cells with exogenous insulin. CPE protein expression was up-regulated by insulin stimulation in control cells in contrast to a blunted response in the βIRKO cells (Fig. 2*A*), confirming that insulin signaling directly modulates the expression of CPE. A previous study has shown that transcription of CPE is positively regulated by insulin via FoxO1 in the proopiomelanocortin (*Pomc*)-expressing neurons (25). To investigate whether CPE is indeed regulated by a similar mechanism in β cells, we were surprised to observe that the CPE transcripts showed a trend toward compensatory up-regulation in the βIRKO cells instead of a decrease, as one would predict from the protein expression level and from the previous study (25) (Fig. S2 *A* and *B*). These data suggest that the down-regulation of CPE protein is mediated by a transcription-independent regulation in the β cells by insulin. Further, we confirmed that the observed down-regulation of CPE protein in the βIRKO cells is not due to altered stability of either the CPE transcript or protein (Fig. S2 *C* and *D*) in contrast to the previously reported CPE regulation by palmitate exposure (26). Therefore, these data indicated that CPE is translationally regulated by insulin in the β cells. Indeed, the pulse-labeling analyses revealed reduced biosynthesis of CPE in the βIRKO cells (Fig. 2*B*). To assess the direct regulation of IR signaling on proinsulin-processing enzymes further, especially CPE protein expression, we transiently knocked down the IR in the control cells by infection of shRNA-expressing lentivirus against the IR and examined the levels of proinsulin-processing enzymes over time. The levels of IR began to decrease 32 h after infection and were accompanied by a decrease in CPE protein, but not CPE mRNA, and did not affect PC1/3 or PC2 protein levels (Fig. 2*C* and Fig. S3*A*).

At this point, we considered previous reports that have shown protein biosynthesis is tightly regulated by ER homeostasis (27, 28), and, interestingly, we observed that chronic absence of insulin signaling in the βIRKO cells up-regulates ER stress (Fig. 2*D* and Fig. S3*B*). To determine whether the down-regulation of CPE biosynthesis is a consequence of ER stress in the βIRKO cells, we examined the cells with acute IR knockdown and failed to detect significant changes in ER stress markers before the decrease of CPE after IR knockdown, suggesting that the down-regulation of CPE protein is directly regulated by insulin signaling and is independent of ER stress (Fig. S3*C*). Further, we observed that knocking down proinsulin or reexpressing CPE or IR in βIRKO cells completely alleviated ER stress (Fig. 2*E* and Fig. S4 *A–E*), suggesting that dysfunctional proinsulin processing potentially regulates the ER stress response in β cells. However, we cannot completely rule out the role of ER stress on CPE
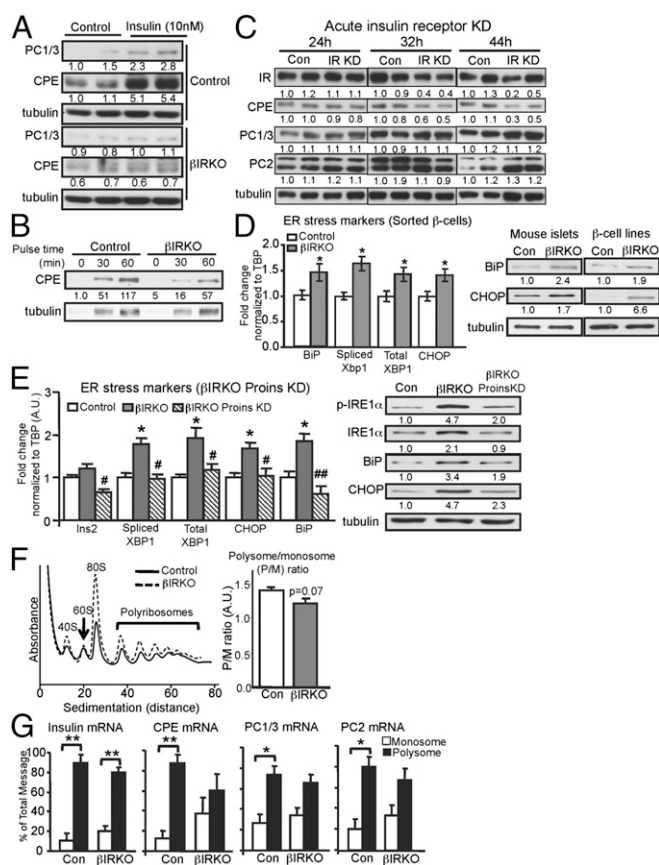

Fig. 2. Insulin signaling regulates CPE translation initiation. (*A*) Western blotting for proinsulin, PC1/3, CPE, and tubulin (loading control) in control or βIRKO cell lines with or without exogenous insulin stimulation (10 nM) for 12 h. (*B*) Western blotting for CPE or tubulin in control or βIRKO cell lines after pulse labeling with modified methionine and then harvesting at the indicated time points. (*C*) Western blotting for IR, CPE, PC1/3, PC2, or tubulin (loading control) in control or IR knockdown (KD) β cells harvested 24, 32, or 44 h after IR shRNA containing lentiviral infection. (*D, Left*) Quantitative PCR (qPCR) for mRNA of ER stress markers (BiP, total XBP-1, spliced XBP-1, or CHOP) in fluorescence-activated cell-sorted β cells from control (open bar) or βIRKO (gray bar) mice (*n* = 4). (*D, Right*) Western blotting for BiP, CHOP, or tubulin (loading control) in islets isolated from control or βIRKO mice and in control or βIRKO cell lines (*n* = 3). (*E, Left*) qPCR for mRNA of ER stress markers (BiP, total XBP-1, spliced XBP-1, and CHOP) in control, βIRKO, or βIRKO proinsulin KD cell lines (*n* = 4 per group). A.U., arbitrary units. (*E, Right*) Western blotting for p-IRE1α, total IRE1α, BiP, CHOP, and tubulin (loading control) in control, βIRKO, or βIRKO proinsulin KD cell lines (*n* = 3 per group). (*F, Left*) Translational profiling of control or βIRKO cells. Profiles through the gradient were measured by A_{254}. Positions of the 40S and 80S subunits, 80S monosome, and polyribosomes are indicated. Data shown are from representative experiments performed on three occasions. (*F, Right*) Polysome/monosome (P/M) ratios for the translational profiles of control or βIRKO cells (*n* = 3). (*G*) Real-time qPCR for insulin, CPE, PC1/3, or PC2 mRNA extracted from pooled monosome or polysome fractions of control or βIRKO cells (*n* = 3). Data are mean ± SEM. *$P < 0.05$ (vs. control); **$P < 0.01$ (vs. control); #$P < 0.05$ (vs. βIRKO); ##$P < 0.01$ (vs. βIRKO).

protein biosynthesis in βIRKO cells secondary to long-term insulin signaling deficiency. Thus, our data confirm a direct role for insulin signaling in CPE protein biosynthesis.

To assess the translational effects of IR KO on CPE transcripts, we performed polyribosomal profiling of total RNA (29). Fig. 2*F* shows the position of the 80S ribosomal species, as well as the polyribosomes from the RNA isolated from control or βIRKO cells. The ratio of polyribosomes to 80S monosomes (P/M ratio) tended to be lower in the βIRKO cells, suggesting

a relative dissipation of the polysome fraction (Fig. 2F). The decrease in polysomes, as reflected in the lower P/M ratio, is characteristic of a block in translational initiation (30). To confirm the block at the transcript level, we analyzed the mRNAs contained in the pooled monosome (nontranslating) and polysome (actively translating) fractions in both control and βIRKO cells. Insulin mRNA preferentially partitioned into polysomes in both cell types (Fig. 2G), suggesting that insulin mRNA is actively translated. Consistently, CPE mRNA is also preferentially partitioned into the polysome fraction in the control cells; however, in contrast, CPE mRNA in the βIRKO cells was observed to partition equally into monosome and polysome pools, suggesting relative translation initiation blockade for CPE. Notably, we did not observe a similar block in translation initiation for the mRNAs encoding PC1/3 and PC2 (Fig. 2G). We observed an unaltered mRNA partitioning for insulin mRNA, which is the most abundant transcript in β cells and other processing enzymes (PC1/3 and PC2). Thus, our data argue for a selective translational initiation regulation of the proinsulin-processing enzyme, CPE, but against a global down-regulation of translation initiation in the βIRKO cells as suggested by the low P/M ratio.

Insulin Signaling Directly Regulates the Translation Initiation Complex to Have an Impact on CPE Translation. To investigate further how insulin regulates the translational process and to identify its translational targets in β cells, we examined the expression pattern of multiple proteins involved in the regulation of protein translation, some of which have been reported to be regulated by insulin signaling, including those in the mammalian target of rapamycin (mTOR) signaling pathways and translation initiation complexes (31). Although a majority of the proteins, including those in the mTOR signaling pathway, such as the 4EBP and eIF2a proteins and most translation initiation complex proteins, were unaffected (Fig. S5A), the translation initiation scaffolding proteins eIF4G1 and eIF4G2 were altered only in the βIRKO cells but not in controls (Fig. 3A). Indeed, in support of a direct effect of insulin, the decrease in expression of IR after knockdown was accompanied by a down-regulation of eIF4G1 as early as 32 h followed later by a decrease in eIF4G2, suggesting secondary regulation of the latter protein by insulin signaling (Fig. 3B). Similar to the observation in βIRKO cells, we observed no significant changes in proteins in the mTOR signaling pathway or translation initiation complexes in cells with acute knockdown of the IR, confirming a specific regulation of eIF4G1 by insulin signaling (Fig. S5B). More importantly, we detected down-regulation of eIF4G1 in islets from HFD mice (Fig. 3C) and islets from patients with T2D (Fig. 3D), confirming the pathophysiological relevance of our observations. Transient reexpression of eIF4G1 restored the protein level of CPE and the proinsulin-to-insulin ratio, confirming the role of eIF4G1 in the regulation of CPE protein level in βIRKO cells and mouse islets isolated from obese ob/ob mice (Fig. 3 E and F).

The efficiency of translation initiation is greatly affected by the mRNA 5′ untranslated region (UTR) harboring a high degree of secondary structure characterized by a high guanine cytosine (GC) content and thermostability [low delta G (dG)] (32). To investigate the mechanism underlying the specific regulation of CPE but not PC1/3 protein expression via down-regulation of eIF4G1 in the insulin signaling-deficient β cells, we examined the 5′ UTR of both CPE and PC1/3 mRNA. Interestingly, despite similarities in length, the 5′ UTR of CPE is relatively GC-rich (71.4% vs. 48%) and has higher energy (dG = −39.64 vs. −17.13), as determined by UNAFold (33), compared with the 5′ UTR of PC1/3 (Fig. 3G). These data predict that the 5′ UTR of the CPE can form a more stable secondary stem loop structure that is subjected to translational initiation regulation compared with PC1/3. This is because eIF4G1 acts as a core scaffolding protein for the critical translation initiation complex, eIF4F, that mediates the initiation of cellular mRNA translation (34). For
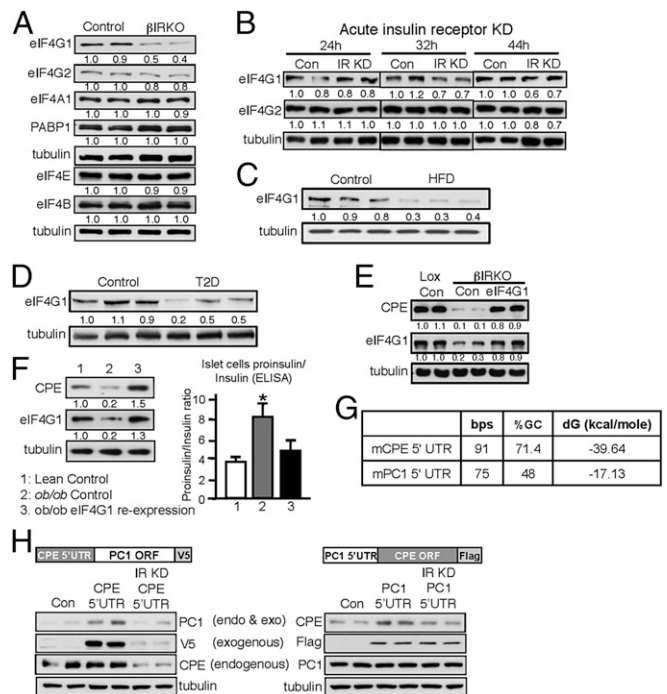

Fig. 3. Insulin signaling regulates the translation initiation complex to modulate CPE translation. (A) Western blotting for eIF4G1, eIF4G2, eIF4A1, polyadenylate-binding protein 1 (PABP1), eIF4E, eIF4B, or tubulin (loading control) in control or βIRKO cells under basal conditions (n = 3). (B) Western blotting for eIF4G1, eIF4G2, or tubulin (loading control) in control or IR KD β cells harvested 24, 32, or 44 h after IR shRNA containing lentiviral infection. (C) Representative Western blotting for eIF4G1 or tubulin (loading control) in islets (pooled) isolated from control or HFD-fed C57BL/6J mice (n = 6). (D) Representative Western blotting for eIF4G1 or tubulin (loading control) in islets isolated from controls or patients with T2D (n = 5). (E) Western blotting for CPE, eIF4G1, and tubulin (loading control) in control, βIRKO, or βIRKO eIF4G1-reexpressing cell lines. (F) Western blotting for CPE, eIF4G1, and tubulin (loading control) (Left) and proinsulin ELISA (Right) in islets isolated from lean control or obese ob/ob mice with or without eIF4G1 reexpression. (G) Length, percentage of GC, dG of CPE, or PC1/3 5′ UTR was analyzed with UNAFold. (H, Left) Western blotting for PC1/3, V5, CPE, or tubulin (loading control) in control, V5 tag-PC1/3 with CPE 5′ UTR, or V5-tag PC1/3 with CPE in IR KD cells. (H, Right) Western blotting for CPE, FLAG, PC1/3, and tubulin (loading control) in control, FLAG-tag-CPE with PC1/3 5′ UTR, or FLAG tag-CPE with PC1/3 5′ UTR in IR KD cells.

example, in the case of CPE, down-regulation of eIF4G1 in βIRKO is expected to reduce the activity of the eIF4F complex, rendering the mRNA with relative highly structured 5′ UTR to translational initiation inhibition. To confirm the role of CPE 5′ UTR on the expression of CPE further, we fused the CPE and PC1/3 open reading frames (ORFs) with PC1/3 and CPE 5′ UTR, respectively. To distinguish exogenously expressed CPE and PC1/3, the ORFs were tagged with FLAG or V5 epitopes, respectively. We observed that the V5-tag PC1/3 with CPE 5′ UTR is overexpressed in the control cells but is down-regulated upon knockdown of the IR, as demonstrated by immunoblotting for PC1/3 (detects both endogenous and exogenous PC1/3) and V5 (detects exogenous PC1/3) (Fig. 3H, Left). Consistently, we also observed down-regulation of the endogenous level of CPE in the cells with knockdown of the IR (Fig. 3H, Left). Similarly, the FLAG-tagged CPE with PC1/3 5′ UTR is overexpressed in the control cells but remains unchanged after knockdown of IR, as shown by the FLAG immunoblot (Fig. 3H, Right). Reduced CPE levels shown by the CPE immunoblot (detects both endogenous and exogenous CPE) are contributed by the reduction of endogenous CPE upon IR knockdown (Fig. 3H, Right), and

endogenously expressed PC1/3 consistently showed no change. Taken together, our data demonstrate that insulin signaling directly modulates the key proinsulin-processing enzyme, CPE, by regulating the translational initiation complex scaffolding protein, eIF4G1.

Transcription Factor Pdx1 Regulates eIF4G1 in Pancreatic β Cells. To investigate the underlying molecular mechanism(s) regulating the level of eIF4G1, we focused on the significant decrease in its gene expression in both βIRKO cells and primary islets (Fig. 4A), which suggested that eIF4G1 is transcriptionally regulated. These alterations were confirmed in primary HFD mouse islets (Fig. 4B) and T2D human islets (Fig. 4C). Next, using in silico sequence analyses, we identified putative binding sites for the pancreatic and duodenal homeobox protein, Pdx1, a critical transcription factor for β-cell survival and function, in the promoter of the murine eIF4G1 gene (Fig. S6A). Consistent with our previous report (17), Pdx1 was down-regulated in both the

β-cell line and primary islets isolated from βIRKO mice (Fig. 4D), as well as in HFD mouse islets (Fig. 4E) and T2D human islets (Fig. 4F). To confirm the role of Pdx1 on eIF4G1 regulation, we examined previously published Pdx1 ChIP sequencing data (35) and observed that Pdx1 binding is enriched at the 5′ region of the eIF4G1 gene locus in both mouse and human primary islet samples (Fig. S6B). This observation was confirmed by Pdx1 ChIP on primary mouse islets, where we detected an approximately fivefold enrichment of Pdx1 binding on both the 5′ and 3′ regions of the eIF4G1 gene (Fig. 4G). Taken together, our data so far suggest that Pdx1 modulates eIF4G1 gene expression via binding at the promoter and potential 3′ enhancer region in β cells and that this regulation is conserved in human islets, as demonstrated in the ChIP-sequencing data. Further experiments that address effects of mutational analyses of the Pdx1 binding site would be necessary to provide evidence for direct regulation of the eIF4G1 gene.

Next, to determine the role of Pdx1 in the regulation of eIF4G1, we transiently reexpressed Pdx1 in the βIRKO cells and mouse islets isolated from obese *ob/ob* mice. Real-time PCR, Western blot, and proinsulin ELISA analysis revealed that Pdx1 reexpression only partially restored the expression of eIF4G1 but completely restored the proinsulin-to-insulin ratio (Fig. 4 H and I), suggesting an additional regulator of eIF4G1 other than Pdx1 in βIRKO cells. To confirm this possibility, we performed acute knockdown of the IR in control cells and observed that Pdx1 expression was significantly down-regulated 44 h after infection (Fig. 4J) and occurred later than down-regulation of eIF4G1 (Fig. 3B).

Transcription Factor SREBP1 Regulates eIF4G1 in Pancreatic β Cells. To identify the additional regulator of eIF4G1, we again analyzed the promoter region of the murine eIF4G1 gene and detected multiple SREBP1 transcription factor binding sites (Fig. 5A) that were highly conserved between murine and human orthologs (Fig. S7A). Indeed, overexpression or activation of SREBP1 has been implicated in the down-regulation of key β-cell genes, including Pdx1, in addition to modulating β-cell function (36, 37). A potential role for SREBP1 in our studies was confirmed by a significant increase in mature SREBP1 in both β-cell lines and primary islets from βIRKO mice (Fig. 5B), as well as in primary islets from HFD mice and humans with T2D (Fig. 5C). A similar increase in mature SREBP1 in the control cells with acute knockdown of the IR (Fig. 5D) suggested direct regulation of SREBP1 by insulin signaling. To confirm the impact of SREBP1 on eIF4G1 expression, we performed acute knockdown of SREBP1 in βIRKO cells. Transient knockdown of SREBP1 (~70%) fully restored the expression of eIF4G1 in the βIRKO cells (Fig. 5E). Further, knockdown of SREBP1 also restored the expression of Pdx1 in the βIRKO cells (Fig. 5E, Lower), confirming a role for SREBP1 in regulating Pdx1 expression (36). Taken together, our data reveal that in the β cells, insulin signaling regulates translation initiation by regulating the level of eIF4G1 via SREBP1 and Pdx1.

To investigate how insulin up-regulates mature SREBP1 in βIRKO cells, we examined the transcription of the full-length SREBP1 and the SREBP1 interacting partners, because transcriptionally active SREBP1 requires processing at the ER and Golgi, which, in turn, is regulated by the availability of its interacting partners, the sterol regulatory element-binding protein cleavage-activating protein (SCAP) and insulin-induced gene (Insig) proteins, at the ER (38). Consistently, the SREBP1 gene expression was also up-regulated in the βIRKO cells (Fig. 5F), as well as in HFD mouse islets and T2D human islets (Fig. 5G). Further, the gene and protein expression of SCAP was up-regulated in both the βIRKO cells and islets (Fig. 5 H and I). Interestingly, we observed an increase in the gene expression of Insig1 and Insig2 in the βIRKO cells but a decrease in its protein levels in both the βIRKO cells and isolated islets (Fig. 5 H and I).
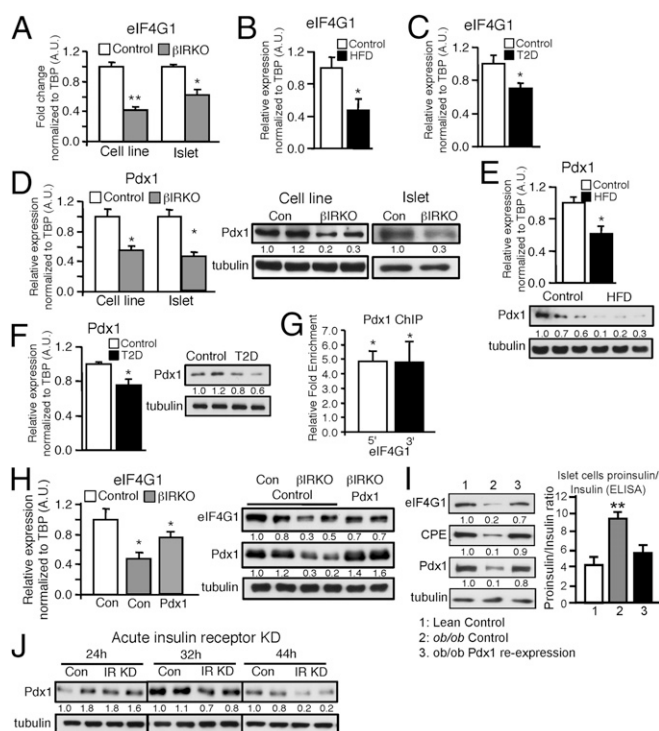

Fig. 4. Insulin signaling regulates eIF4G1 via Pdx1. (A) Real-time qPCR for eIF4G1 in control or βIRKO cell lines and in islets isolated from control or βIRKO mice (n = 4). Data are mean ± SEM. *P < 0.05; **P < 0.01. (B) qPCR for eIF4G1 in islets isolated from control or HFD-fed C57BL/6J mice (n = 6). Data are mean ± SEM. *P < 0.05. (C) qPCR for eIF4G1 in islets isolated from controls or patients with T2D (n = 5). Data are mean ± SEM. *P < 0.05. (D) qPCR (Left) and Western blotting (Right) for Pdx1 in control or βIRKO cell lines and in islets isolated from control or βIRKO mice (n = 4). Data are mean ± SEM. *P < 0.05. (E) qPCR (Upper) and representative Western blotting (Lower) for Pdx1 in islets (pooled) isolated from control or HFD-fed C57BL/6J mice (n = 6). Data are mean ± SEM. *P < 0.05. (F) qPCR (Left) and representative Western blotting (Right) for Pdx1 in islets isolated from controls or patients with T2D (n = 5). Data are mean ± SEM. *P < 0.05. (G) ChIP assay for Pdx1 on eIF4G1 5′ and 3′ regions in primary mouse islets. Data are mean ± SEM. *P < 0.05. (H) qPCR (Left) for eIF4G1 and Western blotting (Right) for eIF4G1, Pdx1, and tubulin (loading control) in control, βIRKO, or βIRKO Pdx1-reexpressing cell lines. (I) Western blotting for CPE, eIF4G1, Pdx1, and tubulin (loading control) (Left) and proinsulin ELISA (Right) in islets isolated from lean control or obese *ob/ob* mice with or without Pdx1 reexpression. (J) Western blotting for Pdx1 or tubulin (loading control) in control or IR KD β cells harvested 24, 32, or 44 h after IR shRNA containing lentiviral infection.
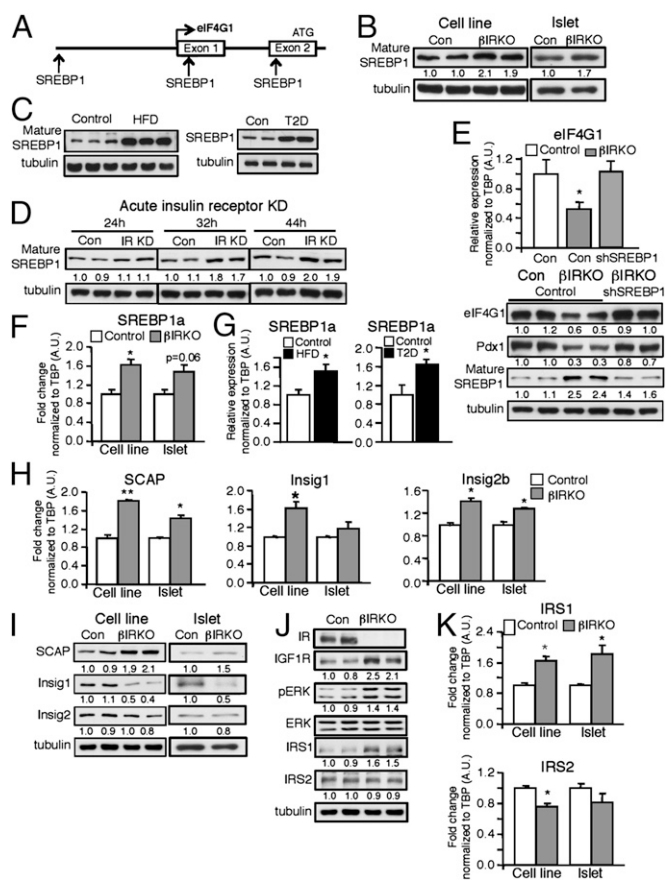
Fig. 5. Insulin signaling regulates eIF4G1 via SREBP1. (*A*) Schematic depicts putative SREBP1 binding sites on eIF4G1 promoter. (*B*) Western blotting for mature SREBP1 or tubulin (loading control) in control or βIRKO cell lines and in islets isolated from control or βIRKO mice (*n* = 3). (*C*) Representative Western blotting for mature SREBP1 or tubulin (loading control) in islets (pooled) isolated from control or HFD-fed C57BL/6J mice (*n* = 6) (*Left*) or from controls or patients with T2D (*n* = 5) (*Right*). (*D*) Western blotting for SREBP1 or tubulin (loading control) in control or IR KD β cells harvested 24, 32, or 44 h after IR shRNA containing lentiviral infection. (*E*) qPCR (*Upper*) for eIF4G1 and Western blotting (*Lower*) for eIF4G1, Pdx1, SREBP1, or tubulin (loading control) in control, βIRKO, or βIRKO SREBP1 KD cell lines. (*F*) qPCR for SREBP1a in control or βIRKO cell lines and in islets isolated from control or βIRKO mice (*n* = 4). Data are mean ± SEM. *$P < 0.05$. (*G*) qPCR for SREBP1a in islets isolated from control or HFD-fed C57BL/6J mice (*n* = 6) (*Left*) or from controls or patients with T2D (*n* = 5) (*Right*). Data are mean ± SEM. *$P < 0.05$. (*H*) qPCR for SCAP (*Left*), Insig1 (*Center*), or Insig2b (*Right*) in control or βIRKO cell lines and in islets isolated from control or βIRKO mice (*n* = 4). Data are mean ± SEM. *$P < 0.05$; **$P < 0.01$. (*I*) Western blotting for SCAP, Insig1, Insig2, or tubulin (loading control) in control or βIRKO cell lines and in islets isolated from control or βIRKO mice (*n* = 3). (*J*) Western blotting for IR, IGF1R, phospho-ERK, total ERK, IRS1, IRS2, or tubulin (loading control) in control or βIRKO cell lines under basal conditions (*n* = 3). (*K*) qPCR for IRS1 (*Upper*) or IRS2 (*Lower*) in control or βIRKO cell lines and in islets isolated from control or βIRKO mice (*n* = 4). *$P < 0.05$.

This observation is consistent with a previous study (39), which reported that degradation of Insig1, a protein with a short $t_{1/2}$, is accelerated in cells with induced ER stress such as occurs in the βIRKO cells (Fig. S3*B*). Up-regulation in Insig1 mRNA is likely a compensatory response for the reduced protein levels in the ER. Taken together, our observations indicate that an increase in mature SREBP1 in βIRKO cells and islets is potentially due to an increase in SREBP1 and SCAP expression, and is facilitated by the down-regulation of Insig1 protein.

From the literature, it is evident that insulin potently stimulates SREBP1 gene expression via a "feed-forward" mechanism

in the liver (40, 41). However, in this study, interestingly, we observed an up-regulation of SREBP1 gene expression in the β cells despite the absence of functional IRs. This observation is analogous to the pathophysiological phenomenon wherein SREBP1 is up-regulated in insulin-resistant hepatocytes (42); however, this has not, to our knowledge, been described in the pancreatic β cell. To investigate the potential mechanism underlying our observation, we examined insulin signaling in the βIRKO cells. Under basal conditions, we observed an increase in phospho-ERK with unchanged phospho-Akt (Fig. 5*J* and Fig. S7*B*), which is probably due to a compensatory up-regulation of insulin-like growth factor 1 receptors (IGF1Rs) in the IR-deficient β-cell line, a finding we have reported previously (18, 20). These data suggest that up-regulation of the ERK pathway in the βIRKO cell is sufficient to restore specific insulin signaling functions that are especially relevant for the regulation of SREBP1 expression. We also observed an increase in the gene and protein expression of IR substrate-1 (IRS1) and a decrease in IRS2 mRNA but unchanged IRS2 protein levels in the βIRKO cells (Fig. 5 *J* and *K*). Indeed, previous studies in the liver have reported that IRS1, but not IRS2, is positively correlated with the expression of SREBP1c (43) and that insulin acts via IRS1 to stimulate SREBP1-regulated lipogenic genes in the liver (44). Our results demonstrate that in the insulin signaling-deficient β cells, a selective up-regulation of IRS1 leads to an increase in SREBP1 and a subsequent decrease in Pdx1 protein that ultimately inhibits proinsulin processing by suppressing translation initiation.

Discussion

Elevated levels of proinsulin and proinsulin intermediates are features of T2D (2) and are strongly associated with impaired β-cell function and development of the disease in humans (45, 46). In this study, we report a novel link between IR growth factor signaling, translational initiation, and proinsulin processing in pancreatic β cells.

Previously, we have reported that insulin signaling affects β-cell proliferation, survival, and secretory function (reviewed in ref. 22). An increase in circulating proinsulin in the βIRKO mice led us to hypothesize that insulin signaling regulates proinsulin processing. Our finding on proinsulin accumulation in β cells lacking IRs is similar to that in mice with KO of the individual proinsulin-processing enzymes PC1/3, PC2, or CPE, all of which exhibit increased circulating proinsulin (47–50). Higher circulating proinsulin in βIRKO mice and increased proinsulin content in βIRKO cells are due to defective proinsulin processing secondary to a decrease in the eukaryotic initiation factor eIF4G1 and subsequent down-regulation of CPE biosynthesis. Higher circulating proinsulin in βIRKO mice could potentially be due to an increase in the constitutive secretory pathway in βIRKO cells, because CPE has been shown to function as a prohormone sorting receptor (51). Down-regulation of CPE in βIRKO cells could potentially fail to direct proinsulin to the regulated secretory pathway; however, an increase in circulating proinsulin in βIRKO mice was accompanied by an increase in proinsulin content in βIRKO cells, which argues against a role for the constitutive secretory pathway.

The decrease in CPE levels in the βIRKO islets and cells is consistent with an increase in circulating split proinsulin intermediate in patients with T2D (45). Suppressed CPE expression, due to a significant alteration in protein biosynthesis, was particularly dramatic in the βIRKO cells, which demonstrated specific partitioning of CPE mRNA into monosomes. Our finding is in contrast to that of a previous study showing that CPE protein in β cells is down-regulated by palmitate exposure via a mechanism involving protein degradation (26). Because insulin resistance and dyslipidemia are both risk factors for T2D, biosynthesis and stability of CPE could be one of the key regulatory

mechanisms modulating CPE levels in β cells in determining the onset and progression of the disease.

Because mice with mutations in the coding region of the CPE gene (Cpe*fat* mice) (48) also exhibit alterations in PC1/3 and PC2 expression in the pituitary (52) and processing of other hypothalamic peptides (53), the direct effects of the very low levels of CPE on expression of PC1/3 in the βIRKO model cannot be ruled out.

The direct link between insulin signaling, translation initiation, and processing enzymes is evident by a coordinated down-regulation of eIF4G1 and CPE upon acute down-regulation of IR in control β cells. Insulin signaling regulates protein translation via the mTOR signaling pathway and by phosphorylation of certain translation initiation proteins (31). It is also known that protein synthesis is primarily regulated at the translation initiation step (rather than during elongation or termination), allowing rapid, reversible, and spatial control of gene expression. This regulation occurs by means of both the cis-regulatory elements, such as the 5′ and 3′ UTRs, and the transacting factors (54). Thus, the highly structured UTRs with GC-rich sequences, upstream ORFs, and internal ribosome entry site could all significantly influence the rate of translation. A breakdown in this regulatory machinery could perturb cellular metabolism, leading to significant physiological abnormalities (55, 56).

We show that insulin signaling regulates eIF4G1, leading to down-regulation of the CPE proinsulin-processing enzyme, which exhibits a more structured 5′ UTR. eIF4G1 is a core scaffolding protein for the critical translation initiation complex, eIF4F, that regulates the translation initiation of mRNAs encoding mitochondrial, cell survival, and growth genes in response to diverse stressors (55). The efficiency of translation initiation is known to be greatly affected by the complexity of the mRNA 5′ UTR secondary structures. As such, 5′ UTRs harboring a high degree of secondary structure (e.g., high GC content) and thermostability (low dG) are often highly dependent on eIF4F complex translational activity (32). Down-regulation of eIF4G1 in βIRKO is expected to reduce the activity of the eIF4F complex.

β cells with a reduced complement of functional IRs exhibit reduced expression of the homeodomain protein, Pdx1 (17), a critical transcription factor that regulates β-cell development and function (57). In this study, we also showed that Pdx1 is down-regulated in islets from patients with T2D and in primary islets isolated from HFD mice, a commonly used T2D rodent model. Identification of Pdx1 binding sites on the promoter region of the eIF4G1 gene suggested a potential role for Pdx1 in the expression of eIF4G1. This was confirmed by examination of previously published Pdx1 cistrome datasets for human and mouse islets (35) and by Pdx1 ChIP using primary mouse islets. Indeed, restoration of Pdx1 levels in the βIRKO cells partially recovered the expression of eIF4G1, suggesting that the homeodomain protein regulates translational initiation in the IR KO β cells. This observation led us to identify another transcription factor in the regulation of translation initiation in the β cell.

SREBP1 is a transmembrane basic helix–loop–helix leucine zipper family of transcription factor proteins of the ER. It is well characterized that SREBPs activate the synthesis of fatty acids, triglycerides, and cholesterol in the liver (38). In contrast, the role of SREBP in β cells is poorly understood. A limited number of studies have reported that activation of SREBP1 in β cells is associated with impaired insulin secretion, enhanced apoptosis, and suppression of critical genes involved in β-cell function, including Pdx1 and IRS2, together leading to β-cell dysfunction (36). In our study, we observed that expression of both Pdx1 and IRS2 is down-regulated in the βIRKO cell, which could be due, in part, to up-regulated SREBP1, because knocking down SREBP1 in the βIRKO cell restored expression of Pdx1.

Despite being regulated by insulin, SREBP1 was reported to be elevated in insulin resistance in the liver (42). Although the mechanism underlying this selective insulin resistance is not completely understood, it has been suggested that the Akt arm of the insulin signaling pathway, which mediates metabolic effects of insulin, becomes resistant to insulin, whereas the MAPK arm remains sensitive (58). Indeed, this is exactly what we observed in the βIRKO cells. Our observation of selective activation of the MAPK pathway in insulin-resistant β cells provides a plausible mechanistic link for a recently identified unusually high linkage disequilibrium locus, *MADD*, which was associated with elevated proinsulin level and impaired proinsulin processing (4–6). *MADD* encodes an adaptor protein that plays a role in MAPK activation (59), suggesting that MAPK activation contributes to proinsulin processing in β cells. However, we do not rule out the contribution of a compensatory up-regulation of IGF1R in the βIRKO cells that may contribute to the findings in selective hepatic insulin resistance (42, 58). Up-regulation of Insig1 further supports the notion of selective insulin resistance in the βIRKO cell. Our observations of differential regulation of IRS1 vs. IRS2 levels in the βIRKO cells are consistent with a previous study, which reported that IRS2 is involved in the inhibitory effects on gluconeogenesis in the liver, whereas IRS1 transduces stimulatory effects of insulin on de novo lipogenesis, particularly SREBP1 (44, 60).

The ER plays an important role in insulin biosynthesis, and properly folded proinsulin is delivered to the Golgi to be packaged into secretory granules for conversion into mature insulin (61); therefore, ER homeostasis is known to regulate β-cell function (62). We observed that chronic absence of insulin signaling (e.g., in the βIRKO cell) promotes ER stress, which could potentially contribute to the up-regulation of proinsulin and down-regulation of CPE biosynthesis. However, the results from our acute IR knockdown experiments in control β cells suggest that the down-regulation of CPE protein is not caused by ER stress, because no significant changes in ER stress markers were detected before a decrease in CPE levels after knockdown of the IR. However, whether CPE is affected by ER stress secondary to long-term insulin signaling deficiency requires further work.

In summary, we provide evidence that compromised insulin signaling in pancreatic β cells coordinately regulates Pdx1 and SREBP1, leading to down-regulation of eIF4G1 and selective inhibition of CPE translation initiation, which causes defective proinsulin processing and accumulation of circulating proinsulin (Fig. 6A). An increase in circulating proinsulin even before the onset of diabetes in the βIRKO, and potentially in the IRS2KO mouse (24), suggests that proinsulin is a useful biomarker of β-cell dysfunction in this model. Our data indicate that these effects are independent of ER stress, and, importantly, we confirm similar molecular defects in primary islets from insulin-resistant patients with T2D. Whether the molecular defects proposed in our study contribute directly to the generation of proinsulin-related peptides (Fig. 6B) and reduced β-cell mass and whether proinsulin is a reliable biomarker to detect T2D early in the disease process in humans warrant further investigation.

Methods

Preparation of β-Cell Lines. β-cell lines from βIRKO and control mice were generated as described previously (19, 20). All protocols were approved by the Institutional Animal Care and Use Committee of the Joslin Diabetes Center and Brandeis University and were in accordance with National Institutes of Health guidelines.

Cell Culture. Cells were maintained in DMEM containing 25 mM glucose supplemented with 10% (vol/vol) FBS and 100 units/mL penicillin/streptomycin. Experiments were performed using 80–90% confluent cells.

Islet Isolation and Dispersion. Islets were isolated by the intraductal collagenase digestion method, as described previously in 5- to 6-mo-old male mice (19), in HFD chow-fed C57BL/6J or *ob/ob* mice obtained from The Jackson Laboratory. Following overnight culture in RPMI 1640 and 10% (vol/vol) FBS,
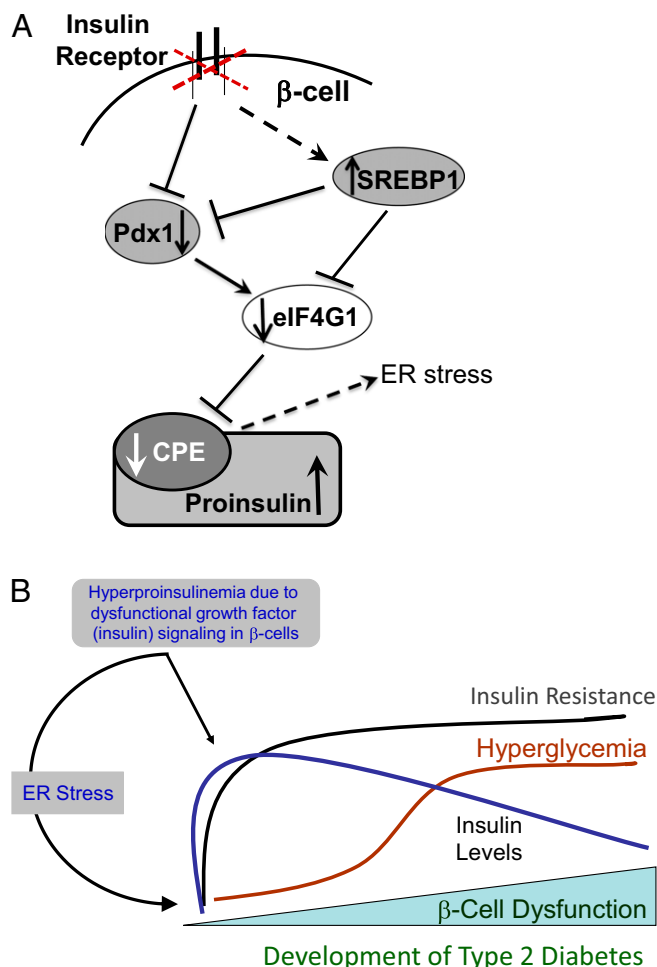
Fig. 6. (*A*) Schematic depicts a potential role for insulin signaling in the regulation of translation initiation, proinsulin processing, and ER stress. (*B*) Hypothetical model shows an early rise in circulating proinsulin levels due to dysfunctional growth factor (insulin) signaling in β cells and ER stress, together contributing to progressive β-cell failure and the development of overt T2D.

7 mM glucose islets were dispersed after washing in PBS, followed by digestion for 15 min in a 37 °C water bath with 1 mg/mL trypsin (Sigma–Aldrich) and 30 units/mL DNase. Digestion was stopped by adding cold DMEM containing 10% (vol/vol) FBS. After several washing steps in PBS, the cell suspension was filtered. Subsequently, fluorescence-activated cell-sorted cells were sorted using autofluorescence and size criteria (63) directly into TRIzol reagent (Invitrogen). The purity of β-cell and non–β-cell fractions was confirmed by real-time PCR for insulin and glucagon, respectively.

Human Islets. All human islets were obtained from the Southern California Islet Resources Center. Upon receipt, all human islets were cultured overnight in Miami Media 1A (Cellgro) before being subjected to experimental procedures as described below. All protocols were approved by the Institutional Review Board of the Joslin Diabetes Center.

Immunohistochemistry. Paraffin-embedded pancreas sections were stained for proinsulin with a mouse monoclonal antibody (gift from Scott Heller, Novo Nordisk, Copenhagen) used at a 1:100 dilution at 4 °C overnight, followed by incubation with FITC-conjugated anti-mouse antibody (1:100 dilution, 1 h at room temperature; Jackson Immunoresearch). For insulin, sections were incubated with antiinsulin antibody (Millipore) at a 1:100 dilution overnight (4 °C), followed by incubation with Texas Red conjugated anti-guinea pig antibody (1:100; Jackson Immunoresearch) for 1 h at room temperature. Slides were examined under an Olympus BX60 optical microscope or Zeiss LSM 710 microscope under confocal mode.

Proinsulin Quantification from Immunohistochemistry. The number of β cells expressing proinsulin was scored in at least 1,000 β cells per mouse and three mice per genotype. The proinsulin-to-insulin cell ratio in controls was arbitrarily set at 1.

SDS/PAGE and Western Blotting. Cultured cells were lysed in radioimmunoprecipitation buffer [150 mM NaCl, 10 mM Tris (pH 7.2), 1% Triton X-100, 1% deoxycholate, 5 mM EDTA] containing 200 μM orthovanadate and protease inhibitors (Sigma–Aldrich) (64). Lysates were precleared at $16,000 \times g$ for 15 min at 4 °C, and total protein concentration was determined using bicinchoninic acid assays (Pierce). Samples were resuspended in reducing SDS/PAGE sample buffer, boiled, and resolved by SDS/PAGE. Proteins were then transferred onto nitrocellulose membranes (Schleicher & Schuell), blocked in 5% (wt/vol) milk in Tris-buffered saline containing 0.1% Tween, and incubated with primary antibodies overnight at 4 °C. PC1/3 and PC2 antibodies are from Affinity BioReagents; CPE, Insig1, and tubulin antibodies are from Abcam; insulin, SREBP1, IR, and IGF1R antibodies are from Santa Cruz Biotechnology; phospho–inositol-requiring enzyme 1α (pIRE1α) antibody is from Novus Biologicals; IRE1α, immunoglobulin-heavy-chain-binding protein (BiP), cleavage and total Caspase 3, phospho-Akt, total Akt, phospho-ERK, total ERK, IRS2 and all translational related antibodies are from Cell Signaling; X-box binding protein-1 (XBP-1), ATF6, and C/EBP homology protein (CHOP) are from Santa Cruz Biotechnology. Pdx1 and IRS1 antibodies are from Millipore, and V5 and Flag antibodies from are GenScript. SCAP antibody is from Proteintech.

For proinsulin processing assays, cells grown in 6-cm plates were lysed in Laemmli sample buffer, sonicated, and heated at 80 °C for 10 min. After electrophoresis through an 8–16% (vol/vol) Tris·glycine gel (Invitrogen), proteins were transferred to a nitrocellulose membrane and probed with anti-GFP rabbit polyclonal antibody (Invitrogen).

Nonradioactive Pulse Labeling. The Click-iT AHA (ʟ-azidohomoalaine) for nascent protein synthesis kit (Invitrogen) was used for these studies, and experiments were performed according to the manufacturer's recommendations. Briefly, cells were seeded into 6-cm plates and allowed to grow to 80–90% confluency. Cells were starved with methionine-free media for 1 h before incubation with Click-iT AHA containing methionine-free media for the indicated time (pulse) before harvesting for analysis. Harvested cells were lysed, cell lysates were labeled with biotin-conjugated alkyne, and biotin-labeled proteins were immunoprecipitated with streptavidin beads and further analyzed by Western blotting.

Real-Time PCR. RNA was extracted using the TRIzol (Invitrogen) method according to the manufacturer's protocol. Following DNase digestion (Ambion), 1 μg of RNA was transcribed into cDNA in a 20-μL reaction (Applied Biosystems). cDNA was analyzed and amplified using the ABI 7900HT system (Applied Biosystems). PCR assays were performed in a 10-μL reaction containing 2.5 μL of cDNA (1:20 diluted), 100 nM primer (each primer), and 1× SYBR Green PCR Master Mix (Applied Biosystems). The expression level of TATA-binding protein (TBP) was used as an internal control. Cycle threshold (Ct) values were used to calculate the amount of amplified PCR product in comparison to the housekeeping gene, TBP. The results are expressed as the fold change in mean ± SEM. The relative amount of each transcript was analyzed using the $2^{-\Delta C(t)}$ method. Statistical differences between mRNA levels were determined using the nonparametric Student's *t* test. A two-sided *P* value <0.05 was considered significant.

Primers used were as follows: TGGCTTCTTCTACACACCCAAG and ACAATGCCACGCTTCTGCC for mature insulin 2 mRNA, GGGGAGCGTGGCTTCTTCTA and GGGGACAGAATTCAGTGGCA for insulin 2 pre-mRNA, ACCCTTCACCAATGACTCCTATG and ATGATGACTGCAGCAAATCGC for TBP, CCTCCTACAGCAGTGGTGATTACA and GGGTCTCTGTGCAGTCATTGT for PC1, AGACAATGGGAAGACGGTTG and TTGAAGCATAGCCGTCACAG for PC2, GCTCAGGTAATTGAAGTCTT and TACTGCTCACGAATACAGTT for CPE, CCTGTTGGTGCACTTCCTA and TCTGAAGGTCCCCGGGGCT for insulin 1, TGGTGCTCATCTCGTCAGAG and TGAATTTGAGAGGCATGCTG for glucagon, AATGACATGAAGGAGGCAGTAC and GTGTTTCATACAGCCCTTGATAG for eIF4G1, TCCCAAACAGAAGGAGGATG and CATTCCGGAGGAGAGCTTTTG for IRS1, AGGCAGCGGCAGGTACCTCAG and GTCATGGGCATGTAGCCATCA for IRS2, GGCCGAGATGTGCGAACT and TTGTTGATGAGCTGGAGCATGT for SREBP1a, GAGCCATGGATTGCACATTT and CTCAGGAGAGTTGGCACCTG for SREBP1c, ATGACCCTGACTGAAAGGCTTCGT and TAACCCTTCACAGGCGTGGAGAAT for SCAP, TCACAGTGACTGAGCTTCAGCA and TCATCTTCATCACACCCAGGAC for Insig1, and CCGGGCAGAGCTCAGGAT and GAAGCAGACCAATGTTTCAATGG for Insig2b. ER stress was determined using the following primers: TTCAGCCAATTATCAGCAAACTCT and TTTTCTGATGTATCCTCTTCACCAGT for BiP, CCACCACACCTGAAAGCAGAA and AGGTGAAAGGCAGGGACTCA for Chop,

TGGCCGGGTCTGCTGAGTCCG and GTCCATGGGAAGATGTTCTGG for total XBP-1; and CTGAGTCCGAATCAGGTGCAG and GTCCATGGGAAGAT-GTTCTGG for spliced XBP-1.

For degradation experiments, cells were incubated with 100 μg/mL Actinomycin D to inhibit transcription and harvested at 0, 30, and 60 min. Insulin pre-mRNA and mature RNA were determined by generating specific primer sets that amplify segments of exons to measure spliced and unspliced mRNA (i.e., total mRNA). Those primer sets that amplify segments of introns only or intron/exon boundaries were considered unspliced mRNA (i.e., pre-mRNAs).

Reexpression of IRs in βIRKO Cells. Human IR B isoform was stably introduced into βIRKO cells by retroviral infection. Plates of Phoenix cells were transiently transfected with the retroviral expression vector system pBABE containing human IR cDNA or with empty pBABE vectors (mock controls) using lipofectamine (Invitrogen). After removing the transfection reagent, cells were kept for 48 h at 32 °C. The virus containing supernatant was then removed, filtered, and used to infect cells. After overnight infection, cells were kept in selection media containing 400 μg/mL Hygromycin B.

Lentiviral Knockdown in β Cells. Mouse proinsulin, IR, and SREBP1 shRNA lentivirus construct were obtained from the University of Massachusetts RNAi Core Facility (RNAi Consortium library) or Open Biosystems. Lentivirus particles were generated according to the supplier's recommendations (Open Biosystems). βIRKO cells were plated 24 h before infection with virus particles. Seventy-two hours after infection, cells were harvested for RNA and subjected to protein analyses.

Reexpression of CPE in βIRKO Cells. Human CPE was subcloned from pCMV6-XL5 (Origene) into pCDH-CMV-MSC-EF1-GreenPuro lentiviral vector (System Biosciences). Lentivirus particles were generated according to the manufacturer's recommendations. βIRKO cells were plated 24 h before infection with virus particles. Seventy-two hours after infection, cells were harvested for RNA and protein analyses.

Reexpression of Pdx1 or eIF41 in βIRKO Cells. Mouse complete Pdx1 or eIF4G1 ORF was amplified from MIN6 cDNA with PCR using oligos from Integrated DNA Technologies and cloned into pCDH-CMV-MSC-EF1-GreenPuro lentiviral vector. Lentivirus particles were generated according to the manufacturer's recommendations (System Biosciences). βIRKO cells were plated 24 h before infection with virus particles. Seventy-two hours after infection, cells were harvested for RNA and protein analyses.

Proinsulin and Insulin Measurement. Cells or islets were extracted with acid ethanol [18% (vol/vol) 1N HCl, 75% (vol/vol) ethanol, 7% (vol/vol) H_2O] solution for 16 h at 4 °C. The proinsulin (Alpco) and insulin (Linco) concentration was measured by ELISA. The proinsulin and insulin content was normalized to the total DNA content. For HPLC analyses, size-matched isolated islets were subjected to incubation with 100 mCi of [^{3}H]-leucine in KREB ringer buffer (64) at 37 °C for 1 h. Islets were then extracted with 100 mM HCl and sonicated. Extracted cell lysates were applied to Altima Reverse-Phase C18 (5-μm) HPLC columns with a Beckman–Coulter HPLC System Gold

(islets core facility, The University of Chicago). Protein fractions were eluted and quantified.

Polyribosomal Profiling and Gradient Fraction Quantitative PCR. For polyribosomal profiling studies, βIRKO cells and control cells were lysed and processed for polyribosomal profile analysis on sucrose gradients as described previously (65). A piston gradient fractionator (BioComp) was used to measure RNA A_{254} with an in-line UV monitor, and gradients were collected in ten 1-mL fractions. Fractions 1–5 were combined as the monosome pool, and fractions 6–10 were combined as the polysome pool. RNA was isolated from each pool using the Qiagen RNeasy Plus Mini Kit and subjected to quantitative real-time RT-PCR using SYBR-Green methodology. The percentage of message recovered in the monosome and polysome pools was determined for each condition.

ChIP. Briefly, ~500 islets from 8-wk-old male CD1 mice were isolated, fixed in 1% formaldehyde, and quenched in glycine. Islets were washed with PBS and lysed in 100 μL of cold lysis buffer [10 mM Tris·HCl (pH 8.0), 10 mM NaCl, 3 mM $MgCl_2$, 1% Nonidet P-40, 0.1% SDS, 0.5% deoxycholic acid] with protease and phosphatase inhibitors (Calbiochem) for 10 min. Islets were then sonicated with a Diagenode bioruptor (30-s on/off pulses for a total of 15 min). Immunoprecipitations were performed as previously described (66) using a goat anti-Pdx1 antiserum (kindly provided by C. Wright, Vanderbilt University, Nashville, TN). The ChIP PCR was done with the following primers: eIF4G1 5′F, CCGGAAATGGTTGTGGACTA; eIF4G1 5′R, CGGACATGGCGGCTTTA; eIF4G1 3′F, AATGACTGCATGGTCTACCG; eIF4G1 3′R, GGCAAGCCTACGTCACAG; Alb F, TGGGAAAACCATCCTATCAAA; and Alb R, CACCTCTTTGTTGTTTCCTTCTG.

1. Gorden P, Roth J (1969) Plasma insulin: Fluctuations in the "big" insulin component in man after glucose and other stimuli. *J Clin Invest* 48(12):2225–2234.
2. Kahn SE, Halban PA (1997) Release of incompletely processed proinsulin is the cause of the disproportionate proinsulinemia of NIDDM. *Diabetes* 46(11):1725–1732.
3. Porte D, Jr., Kahn SE (1989) Hyperproinsulinemia and amyloid in NIDDM. Clues to etiology of islet beta-cell dysfunction? *Diabetes* 38(11):1333–1336.
4. Wagner R, et al. (2011) Glucose-raising genetic variants in MADD and ADCY5 impair conversion of proinsulin to insulin. *PLoS ONE* 6(8):e23639.
5. Strawbridge RJ, et al.; DIAGRAM Consortium; GIANT Consortium; MuTHER Consortium; CARDIoGRAM Consortium; C4D Consortium (2011) Genome-wide association identifies nine common variants associated with fasting proinsulin levels and provides new insights into the pathophysiology of type 2 diabetes. *Diabetes* 60(10):2624–2634.
6. Huyghe JR, et al. (2013) Exome array analysis identifies new loci and low-frequency variants influencing insulin processing and secretion. *Nat Genet* 45(2):197–201.
7. Pradhan AD, et al. (2003) Insulin, proinsulin, proinsulin:insulin ratio, and the risk of developing type 2 diabetes mellitus in women. *Am J Med* 114(6):438–444.
8. Zethelius B, Byberg L, Hales CN, Lithell H, Berne C (2003) Proinsulin and acute insulin response independently predict Type 2 diabetes mellitus in men—Report from 27 years of follow-up study. *Diabetologia* 46(1):20–26.
9. Mykkänen L, Zaccaro DJ, Hales CN, Festa A, Haffner SM (1999) The relation of proinsulin and insulin to insulin sensitivity and acute insulin response in subjects with newly diagnosed type II diabetes: The Insulin Resistance Atherosclerosis Study. *Diabetologia* 42(9):1060–1066.
10. Saad MF, et al. (1990) Disproportionately elevated proinsulin in Pima Indians with noninsulin-dependent diabetes mellitus. *J Clin Endocrinol Metab* 70(5):1247–1253.
11. Reaven GM, et al. (1993) Plasma insulin, C-peptide, and proinsulin concentrations in obese and nonobese individuals with varying degrees of glucose tolerance. *J Clin Endocrinol Metab* 76(1):44–48.
12. Davidson HW, Hutton JC (1987) The insulin-secretory-granule carboxypeptidase H. Purification and demonstration of involvement in proinsulin processing. *Biochem J* 245(2):575–582.
13. Bailyes EM, et al. (1992) A member of the eukaryotic subtilisin family (PC3) has the enzymic properties of the type 1 proinsulin-converting endopeptidase. *Biochem J* 285(Pt 2):391–394.
14. Bennett DL, et al. (1992) Identification of the type 2 proinsulin processing endopeptidase as PC2, a member of the eukaryote subtilisin family. *J Biol Chem* 267(21):15229–15236.
15. Zhou A, Webb G, Zhu X, Steiner DF (1999) Proteolytic processing in the secretory pathway. *J Biol Chem* 274(30):20745–20748.
16. Liu M, Wright J, Guo H, Xiong Y, Arvan P (2014) Proinsulin entry and transit through the endoplasmic reticulum in pancreatic Beta cells. *Vitam Horm* 95:35–62.
17. Okada T, et al. (2007) Insulin receptors in beta-cells are critical for islet compensatory growth response to insulin resistance. *Proc Natl Acad Sci USA* 104(21):8977–8982.
18. Liu S, et al. (2009) Insulin signaling regulates mitochondrial function in pancreatic beta-cells. *PLoS ONE* 4(11):e7983.
19. Kulkarni RN, et al. (1999) Tissue-specific knockout of the insulin receptor in pancreatic beta cells creates an insulin secretory defect similar to that in type 2 diabetes. *Cell* 96(3):329–339.
20. Assmann A, Ueki K, Winnay JN, Kadowaki T, Kulkarni RN (2009) Glucose effects on beta-cell growth and survival require activation of insulin receptors and insulin receptor substrate 2. *Mol Cell Biol* 29(11):3219–3228.

21. Otani K, et al. (2004) Reduced beta-cell mass and altered glucose sensing impair insulin-secretory function in betaIRKO mice. *Am J Physiol Endocrinol Metab* 286(1): E41–E49.

22. Assmann A, Hinault C, Kulkarni RN (2009) Growth factor control of pancreatic islet regeneration and function. *Pediatr Diabetes* 10(1):14–32.

23. Leibiger B, et al. (2001) Selective insulin signaling through A and B insulin receptors regulates transcription of insulin and glucokinase genes in pancreatic beta cells. *Mol Cell* 7(3):559–570.

24. Withers DJ, et al. (1998) Disruption of IRS-2 causes type 2 diabetes in mice. *Nature* 391(6670):900–904.

25. Plum L, et al. (2009) The obesity susceptibility gene Cpe links FoxO1 signaling in hypothalamic pro-opiomelanocortin neurons with regulation of food intake. *Nat Med* 15(10):1195–1201.

26. Jeffrey KD, et al. (2008) Carboxypeptidase E mediates palmitate-induced beta-cell ER stress and apoptosis. *Proc Natl Acad Sci USA* 105(24):8452–8457.

27. Ron D, Walter P (2007) Signal integration in the endoplasmic reticulum unfolded protein response. *Nat Rev Mol Cell Biol* 8(7):519–529.

28. Malhotra JD, Kaufman RJ (2007) The endoplasmic reticulum and the unfolded protein response. *Semin Cell Dev Biol* 18(6):716–731.

29. Teske BF, Baird TD, Wek RC (2011) Methods for analyzing eIF2 kinases and translational control in the unfolded protein response. *Methods Enzymol* 490:333–356.

30. Palam LR, Baird TD, Wek RC (2011) Phosphorylation of eIF2 facilitates ribosomal bypass of an inhibitory upstream ORF to enhance CHOP translation. *J Biol Chem* 286(13): 10939–10949.

31. Selvaraj A, Thomas G (2009) Translational control and insulin signaling. *Handbook of Cell Signaling*, eds Bradshaw RA, Dennis EA (Academic, Waltham, MA), 2nd Ed, pp 2295–2300.

32. Svitkin YV, et al. (2001) The requirement for eukaryotic initiation factor 4A (eIF4A) in translation is in direct proportion to the degree of mRNA 5′ secondary structure. *RNA* 7(3):382–394.

33. Markham NR, Zuker M (2008) UNAFold: Software for nucleic acid folding and hybridization. *Methods Mol Biol* 453:3–31.

34. Gingras AC, Raught B, Sonenberg N (1999) eIF4 initiation factors: Effectors of mRNA recruitment to ribosomes and regulators of translation. *Annu Rev Biochem* 68:913–963.

35. Khoo C, et al. (2012) Research resource: The pdx1 cistrome of pancreatic islets. *Mol Endocrinol* 26(3):521–533.

36. Wang H, Kouri G, Wollheim CB (2005) ER stress and SREBP-1 activation are implicated in beta-cell glucolipotoxicity. *J Cell Sci* 118(Pt 17):3905–3915.

37. Shimano H (2007) Sterol regulatory element-binding protein-1c and pancreatic beta-cell dysfunction. *Diabetes Obes Metab* 9(Suppl 2):133–139.

38. Goldstein JL, DeBose-Boyd RA, Brown MS (2006) Protein sensors for membrane sterols. *Cell* 124(1):35–46.

39. Lee JN, Ye J (2004) Proteolytic activation of sterol regulatory element-binding protein induced by cellular stress through depletion of Insig-1. *J Biol Chem* 279(43): 45257–45265.

40. Foretz M, Guichard C, Ferré P, Foufelle F (1999) Sterol regulatory element binding protein-1c is a major mediator of insulin action on the hepatic expression of glucokinase and lipogenesis-related genes. *Proc Natl Acad Sci USA* 96(22):12737–12742.

41. Shimomura I, et al. (1999) Insulin selectively increases SREBP-1c mRNA in the livers of rats with streptozotocin-induced diabetes. *Proc Natl Acad Sci USA* 96(24):13656–13661.

42. Brown MS, Goldstein JL (2008) Selective versus total insulin resistance: A pathogenic paradox. *Cell Metab* 7(2):95–96.

43. Kohjima M, et al. (2008) SREBP-1c, regulated by the insulin and AMPK signaling pathways, plays a role in nonalcoholic fatty liver disease. *Int J Mol Med* 21(4):507–511.

44. Shimomura I, et al. (2000) Decreased IRS-2 and increased SREBP-1c lead to mixed insulin resistance and sensitivity in livers of lipodystrophic and ob/ob mice. *Mol Cell* 6(1):77–86.

45. Porte D, Jr., Kahn SE (2001) beta-cell dysfunction and failure in type 2 diabetes: Potential mechanisms. *Diabetes* 50(Suppl 1):S160–S163.

46. Røder ME, Porte D, Jr., Schwartz RS, Kahn SE (1998) Disproportionately elevated proinsulin levels reflect the degree of impaired B cell secretory capacity in patients with noninsulin-dependent diabetes mellitus. *J Clin Endocrinol Metab* 83(2):604–608.

47. Furuta M, et al. (1997) Defective prohormone processing and altered pancreatic islet morphology in mice lacking active SPC2. *Proc Natl Acad Sci USA* 94(13):6646–6651.

48. Naggert JK, et al. (1995) Hyperproinsulinaemia in obese fat/fat mice associated with a carboxypeptidase E mutation which reduces enzyme activity. *Nat Genet* 10(2): 135–142.

49. Zhu X, et al. (2002) Severe block in processing of proinsulin to insulin accompanied by elevation of des-64,65 proinsulin intermediates in islets of mice lacking prohormone convertase 1/3. *Proc Natl Acad Sci USA* 99(16):10299–10304.

50. Sapio MR, Fricker LD (2014) Carboxypeptidases in disease: Insights from peptidomic studies. *Proteomics Clin Appl*, 10.1002/prca.201300090.

51. Cawley NX, et al. (2012) New roles of carboxypeptidase E in endocrine and neural function and cancer. *Endocr Rev* 33(2):216–253.

52. Berman Y, Mzhavia N, Polonskaia A, Devi LA (2001) Impaired prohormone convertases in Cpe(fat)/Cpe(fat) mice. *J Biol Chem* 276(2):1466–1473.

53. Nillni EA, Xie W, Mulcahy L, Sanchez VC, Wetsel WC (2002) Deficiencies in pro-thyrotropin-releasing hormone processing and abnormalities in thermoregulation in Cpefat/fat mice. *J Biol Chem* 277(50):48587–48595.

54. Livingstone M, Atas E, Meller A, Sonenberg N (2010) Mechanisms governing the control of mRNA translation. *Phys Biol* 7(2):021001.

55. Shi Y, Taylor SI, Tan SL, Sonenberg N (2003) When translation meets metabolism: Multiple links to diabetes. *Endocr Rev* 24(1):91–101.

56. Chatterjee S, Pal JK (2009) Role of 5′- and 3′-untranslated regions of mRNAs in human diseases. *Biol Cell* 101(5):251–262.

57. Babu DA, Deering TG, Mirmira RG (2007) A feat of metabolic proportions: Pdx1 orchestrates islet development and function in the maintenance of glucose homeostasis. *Mol Genet Metab* 92(1-2):43–55.

58. Cusi K, et al. (2000) Insulin resistance differentially affects the PI 3-kinase- and MAP kinase-mediated signaling in human muscle. *J Clin Invest* 105(3):311–320.

59. Kurada BR, et al. (2009) MADD, a splice variant of IG20, is indispensable for MAPK activation and protection against apoptosis upon tumor necrosis factor-alpha treatment. *J Biol Chem* 284(20):13533–13541.

60. Kubota N, et al. (2008) Dynamic functional relay between insulin receptor substrate 1 and 2 in hepatic insulin signaling during fasting and feeding. *Cell Metab* 8(1):49–64.

61. Fonseca SG, Lipson KL, Urano F (2007) Endoplasmic reticulum stress signaling in pancreatic beta-cells. *Antioxid Redox Signal* 9(12):2335–2344.

62. Lipson KL, et al. (2006) Regulation of insulin biosynthesis in pancreatic beta cells by an endoplasmic reticulum-resident protein kinase IRE1. *Cell Metab* 4(3):245–254.

63. Josefsen K, et al. (1996) Fluorescence-activated cell sorted rat islet cells and studies of the insulin secretory process. *J Endocrinol* 149(1):145–154.

64. Liew CW, et al. (2010) The pseudokinase tribbles homolog 3 interacts with ATF4 to negatively regulate insulin exocytosis in human and mouse beta cells. *J Clin Invest* 120(8):2876–2888.

65. Tersey SA, et al. (2012) Islet β-cell endoplasmic reticulum stress precedes the onset of type 1 diabetes in the nonobese diabetic mouse model. *Diabetes* 61(4):818–827.

66. Raum JC, et al. (2006) FoxA2, Nkx2.2, and PDX-1 regulate islet beta-cell-specific mafA expression through conserved sequences located between base pairs -8118 and -7750 upstream from the transcription start site. *Mol Cell Biol* 26(15):5735–5743.